

Monoatomic magnetic interfaces in IrMn/Cr/Co thin films probed by grazing incidence X-ray absorption spectroscopy

I. García-Aguilar and N. M. Souza-Neto

Laboratório Nacional de Luz Síncrotron (LNLS), Campinas, 13084-971 São Paulo, Brazil

G. M. Azevedo, S. Nicolodi, L. G. Pereira, J. E. Schmidt, and J. Geshev
Instituto de Física, UFRGS, Porto Alegre, 91501-970 Rio Grande do Sul, Brazil

C. Deranlot and F. Petroff

Unité Mixte de Physique CNRS/Thales, 91767 Palaiseau and Université Paris-Sud, 91405 Orsay, France

(Dated: August 9, 2021)

We present depth-resolved experimental results on the atomic and electronic structures of the Co-Cr interface on four IrMn/Cr/Co thin films with variable thickness of the Cr layer. Grazing incidence X-ray absorption near edge structure near the Cr K-edge was used, and an Ångstrom resolved depth-profile for this layer was obtained. An interdiffusion between chromium and cobalt layers was observed in all films, being more pronounced for samples with thinner Cr layers, where Cr behaves as an amorphous material. This causes a contraction in coordination distances in Cr near the interface with Co. In this region, a change in the electronic structure of chromium's 3d orbitals is also observed, and it appears that Cr and Co form a covalent bond resulting in a CrCo alloy. *Ab initio* numerical simulations support such an interpretation of the obtained experimental results.

Magnetic thin-film heterostructures have been the most common type of systems used in the exchange bias (EB) phenomenon research. Although the exchange coupling between the ferromagnetic (FM) and antiferromagnetic (AF) materials has been usually considered to be a nearest-neighbor interaction [1–6], long range interactions across a thin spacer layer (SL) in the FM/AF interfaces have also been reported [7]. Theoretical models [8] indicate that the electronic structure is rather important for RKKY-like long-range interactions, which has been supported by experimental results on the dependence of the FM/AF exchange coupling on the spacer layer [7, 9]. Previous studies on IrMn/Cr/Co thin films, in particular, have shown that magnetic phenomena such as EB and rotatable anisotropy may strongly depend on the thickness of the Cr (a weak AF material) spacer layer thickness as well [10]. In the regard of the latter, an important part of magnetic systems research is the detailed characterization of the electronic and atomic structures as a function of the depth on such samples.

Given the layered nature of these samples and the single-element spacer layer, X-ray Absorption Spectroscopy (XAS) proves to be an effective technique due to its chemical selectivity [11]. Using direct incidence XAS it is not possible to probe nanometric penetration depth; instead, it is convenient to use a grazing incidence (GI) geometry since it allows a selective peer into the depth of the sample [12, 13]. For thin film studies, this confinement also has the considerable advantage of minimizing other layers' contributions as well. Near edge structure on XAS (XANES) provides extra sensitivity information on the closest-surrounding atomic arrangement and on density of unoccupied states, i.e., on the

electronic structure. Using XANES combined with the GI geometry, it is possible to obtain detailed information for the atomic, electronic and magnetic structural differences of monoatomic sublayers across the chromium SL.

Here we present a qualitative depth profile of the atomic and electronic structure of the chromium layers in four polycrystalline IrMn/Cr(t_{Cr})/Co thin films, where the Cr thickness t_{Cr} is varied. A systematic scan of these layers was done using GI-XAS spectroscopy in the XANES regime. Based on collected spectra near the chromium edge, the structural information obtained for the Co/Cr interfaces is analyzed. In addition to the experimental results, interface properties were further examined using *ab initio* simulations.

The four thin films with the composition Ru(150 Å)/IrMn(150 Å)/Cr(t_{Cr})/Co(50 Å)/Au(100 Å) were deposited by magnetron sputtering onto Si(100) substrates, where t_{Cr} =2.5, 7.5, 10 and 20 Å. Complete description of the samples' preparation can be found in Ref. [6]. Since the Cr thickness is significantly low for all films, Ångstrom resolution is needed to accurately study the whole chromium layer. We employed GI-XANES for obtaining this resolution using the method described in Ref. [12].

The GI-XANES measurements were performed at the Brazilian Synchrotron Light Laboratory (LNLS), using the XAFS2 beamline. XANES spectra were collected and normalized for all thin films near the Cr K-edge ($E = 5989$ eV). Energy calibration was done using a reference chromium foil. The incident beam with electric field along the thin-film surface plane was focused on the sample with a vertical divergence of about 0.01° , which intensity was monitored using a first ion chamber. The

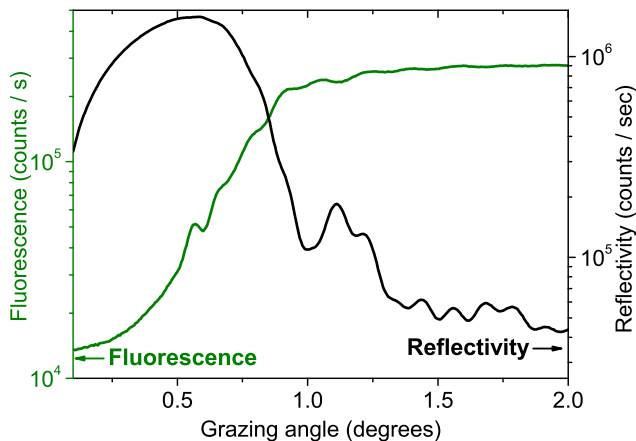


Figure 1: (Color online) Fluorescence and reflectivity data as a function of grazing angle θ , at a fixed energy above the Cr absorption threshold, with approximate maximum absorbance.

reflected beam and the fluorescence emission were simultaneously collected using a second ion chamber and a 15-element Ge detector, respectively. The working grazing-angle calibration was done for every sample using an angular profile at a fixed energy like that shown in Fig.1. The angle values were chosen around the fluorescence decreasing region.

The fluorescence curves used for calibration indicated a complete scan of the chromium layer for all samples when $\theta = 2.0^\circ$. XANES spectra for this grazing angle for each sample are shown in Fig. 2. The low absorption edge from Cr allows for XANES contributions from this layer only, even at high angles. Thicker layers (symbols ■ and □) have a metallic chromium structure which is remarkably different from that of the films with $t_{\text{Cr}} = 2.5$ and 7.5 \AA , where the metallic configuration is lost and more amorphous-like spectra are observed. Since high angle measurements show a convolution of all layers' contributions, in these thinner Cr layers' samples practically the whole Cr layer is interdiffused into the other layers.

The lower inset in Fig. 2 shows a substantial energy shift ($\Delta E \approx 2.5 \text{ eV}$), meaning that near the Cr/Co interface more energy is needed to overcome near atomic potentials [14] which could be interpreted as a contraction in the coordination distances in this top sublayer, and thus an interdiffusion between the chromium and cobalt layers. For samples with thicker Cr layer this interdiffusion is also clearly observed at the Co/Cr interface as will be discussed below.

Besides this change in the absorption edge, there is a progressive decrease in the pre-edge intensity as the chromium layer becomes thinner, and thus as contributions from Cr/Co interface are most appreciable. Given the dependence of the absorption coefficient μ on the density of unoccupied states [11], a drop of the absorption intensity means an increase in occupied states. In

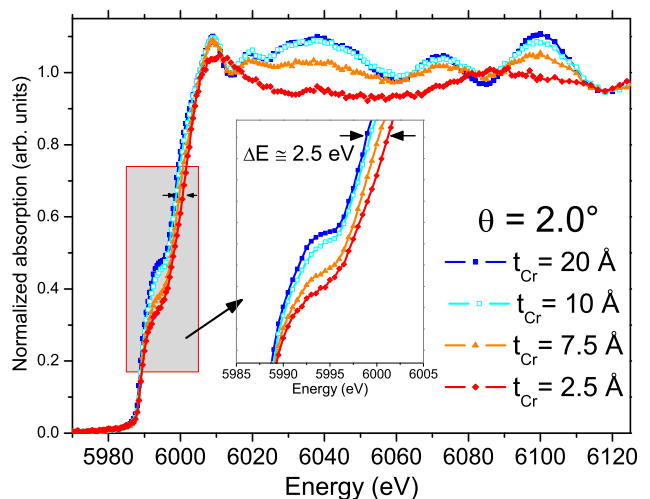


Figure 2: (Color online) Comparison of XANES spectra measured in samples with different Cr layer's thickness in the highest measured angle $\theta = 2.0^\circ$.

XANES, the pre-edge region has a strong contribution from the quadrupole terms ($1s \rightarrow 3d$, in this case), and thus, it probes empty electronic states in $3d$ orbital. Because its intensity decreases in the Cr/Co interface, it appears that chromium ($\text{Cr}:[\text{Ar}]4s^13d^5$) forms a covalent bond with cobalt ($\text{Co}:[\text{Ar}]4s^23d^7$), resulting in an increase in occupied $3d$ states in Cr.

In Fig. 3, the XANES spectra show a qualitative depth profile for $t_{\text{Cr}} = 2.5, 7.5$ and 20 \AA , summarizing differences in electronic and atomic structures in the chromium layer, as a function of its thickness. Similarly to the thickness dependence discussed above, a correlated behavior is found for each sample. Although in Fig. 2 metallic spectra were observed for high angles for $t_{\text{Cr}} = 10$ and 20 \AA , the $\theta = 0.35^\circ$ spectrum (★) in Fig. 3(c) shows the amorphous-like structure and energy shift shows contraction of atomic distances in all plots, meaning that interdiffusion of the chromium and cobalt layers is present in all samples. In the sample with $t_{\text{Cr}} = 10 \text{ \AA}$, the Cr layer is already thick enough to have metallic chromium at the bottom, as evidenced by results equivalent to those shown in Fig. 3(c). For these thicker Cr layer films, the Co-Cr sublayers are considerably thinner as compared to the metallic chromium, thus the contribution from the CrCo alloy is negligible when scanning the whole layer.

No crystalline structure is observed throughout the Cr layer as seen in Fig. 3(a), which shows a complete interdiffusion somewhat expected from the fact that the Cr layer thickness is extremely small as compared to one or two monoatomic layers and that the samples were grown by sputtering. This amorphous behavior is still observed in Fig. 3(b) $\theta < 1.05^\circ$ where EXAFS oscillations are lost in the spectra meaning that the layer interdiffusion has a depth of about 5 \AA . This highlights the resolution strength of the GI-XAS technique in studying thin

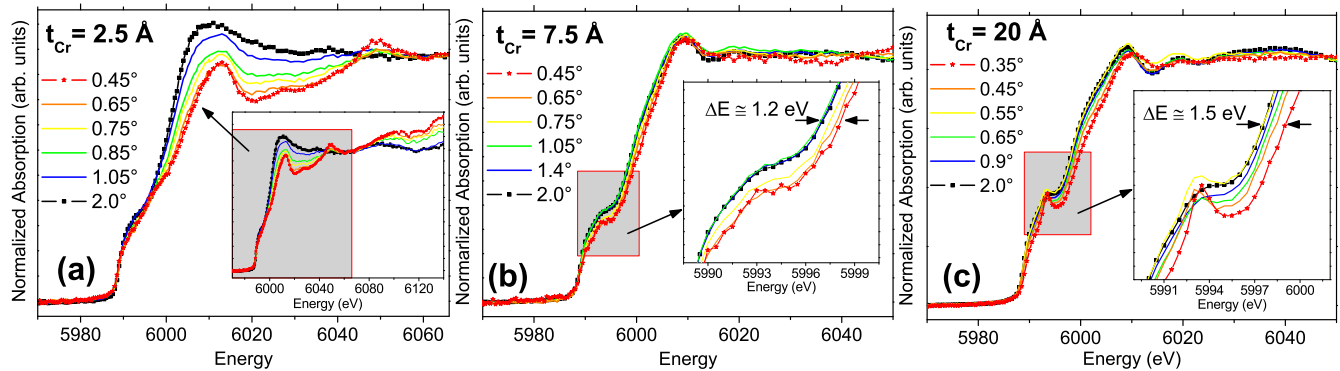


Figure 3: (Color online) XANES spectra as a function of the grazing angle for samples with different Cr layer thicknesses: (a) 2.5 Å, (b) 7.5 Å and (c) 20 Å.

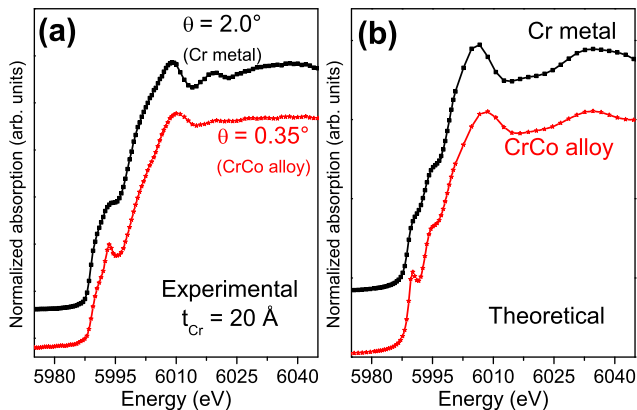


Figure 4: (Color online) (a) Experimental XANES spectra for the sample with $t_{Cr} = 20 \text{ \AA}$ for two grazing angles showing the Co/Cr interface ($\theta = 0.35^\circ$) and a bulk-like metallic Cr character ($\theta = 2.0^\circ$). (b) Numerically-simulated spectra for a metallic Cr bcc lattice and a CrCo alloy with bcc structure with a more contracted lattice.

films and its proficiency in probing monoatomic layers.

The inset in Fig. 3(a) shows a GI geometry effect in XAS. Since the amount of the probed depth is governed by the exponential decay of the incident radiation, the whole 2.5 Å thick Cr layer is probed at any angle/energy but with different weighted contributions. In other words, for low angles, when only the upper region of the Cr layer is being probed, higher energy photons get to penetrate deeper in the layer, which results in a progressive increase in the absorption intensity when increasing the photon energy (as seen in the $\theta = 0.45^\circ$ spectrum (★) for example). At higher angles, this intensity sensitivity on energy becomes insignificant, since X-rays penetrate the whole sample merely because of the geometry itself; a complete scan of the layer is being done in all energies, and the XANES spectra do not show this energy-dependence effect.

The differences in structure between the upper, interdiffused CrCo layer, and the deeper metallic sublayers

are clearer in Fig. 3(c), especially at the pre-edge. These variations are better appreciated in Fig. 4(a), that shows the experimental spectra measured in the lowest and highest angles only; thus, the interface structure as interpreted above is a CrCo alloy and metallic chromium. To support this interpretation *ab initio* simulations using FDMNES code [15] were performed in order to account for a bcc Cr metal structure and a bcc CoCr alloy with smaller interatomic distance, based on the interdiffusion contraction of chromium. Numerical results are shown in Fig. 4(b) for metallic Cr and a CrCo alloy. In both experimental and simulated data, there it is a smoothening of the amorphous spectra (★) past the absorption edge when comparing them with the metallic ones (■). A consequential similarity between them is the appearance of a peak in the pre-edge region due to 3d orbital's changes in agreement with different electronic structures in Cr at the Co-Cr interface resulting from a covalent bond with Co. Besides this, the energy shift associated to the lattice contraction and present in all samples is also found theoretically in the calculated spectra. As a whole, the theoretical simulations agree well with the interpretation of experimental results.

In summary, GI-XANES near chromium K-edge was used to develop Ångstrom resolved depth profiles of electronic and atomic structures on magnetic Co/Cr (t_{Cr})/IrMn films near the Co-Cr interface, as a function of the chromium layer thickness. Interdiffusion between the chromium and cobalt layers was observed for all samples, resulting in a loss of the crystalline structure near the interface. In the samples with thinner Cr layer, i.e. $t_{Cr} = 2.5$ and 7.5 \AA , the whole Cr layers lose the bcc structure behaving as amorphous material, whereas for bigger t_{Cr} low angle spectra evince an interdiffusion of 5 Å in depth. This causes a contraction in the coordination distances near the Co-Cr interface. In this region, there seems that Cr forms a covalent bond with Co as suggested by a change in the electronic structure of chromium 3d orbitals in the Cr XANES pre-edge, which results in a CrCo

alloy. Numerical simulations for a bcc CrCo structure showed consistency with the measured spectra. XANES spectroscopy in the grazing incidence geometry proved to be an efficient technique for an accurate study of these magnetic thin film.

We thank the financial support from the Brazilian agencies CNPq, CAPES and FAPERGS.

-
- [1] L. Thomas, A. J. Kellock, and S. S. P. Parkin, *J. Appl. Phys.* **87**, 5061 (2000).
- [2] T. Mewes, B. F. P. Roos, S. O. Demokritov, and B. Hillebrands, *J. Appl. Phys.* **87**, 5064 (2000).
- [3] M. Gruyters, M. Gierlings, and D. Riegel, *Phys. Rev. B* **64**, 132401 (2001).
- [4] J. Wang, *J. Appl. Phys.* **91**, 7236 (2002).
- [5] Y. G. Yoo, S. G. Min, and S. C. Yu, *J. Mag. Magn. Materials* **304**, e718 (2006).
- [6] J. Geshev, S. Nicolodi, L. G. Pereira, L. C. C. M. Nagamine, J. E. Schmidt, C. Deranlot, F. Petroff, R. L. Rodrigues-Suarez, and A. Azevedo, *Phys. Rev. B* **75**, 214402 (2007).
- [7] N. J. Gökemeijer, T. Ambrose, and C. L. Chien, *Phys. Rev. Lett* **79**, 4270 (1997).
- [8] S. Blundell, *Magnetism in Condensed Matter* (Oxford University Press, 2001).
- [9] S. Nicolodi, L. C. C. M. Nagamine, A. D. C. Viegas, J. E. Schmidt, L. G. Pereira, C. Deranlot, F. Petroff, and J. Geshev, *J. Mag. Magn. Materials* **316**, e97 (2007).
- [10] S. Nicolodi, L. G. Pereira, A. Harres, G. M. Azevedo, J. E. Schmidt, I. Garcia-Aguilar, N. M. Souza-Neto, C. Deranlot, F. Petroff, and J. Geshev, *Phys. Rev. B* **85**, 224438 (2012).
- [11] A. Bianconi, *D. C. Koningsberger and R. Prins (editors). X-Ray Absorption: Principles, Applications, Techniques of EXAFS, SEXAFS and XANES - Chapter 11: XANES Spectroscopy* (John Wiley and Sons, 1988), vol. 92 of *Chemical Analysis*, chap. 11, pp. 573–662.
- [12] N. M. Souza-Neto, A. Y. Ramos, H. C. N. Tolentino, A. Martins, and A. D. Santos, *J. Appl. Cryst.* **42**, 1158 (2009).
- [13] N. M. Souza-Neto, A. Y. Ramos, H. C. N. Tolentino, A. Martins, and A. D. Santos, *Applied Physics Letters* **89**, 111910 (2006).
- [14] N. Souza-Neto, A. Ramos, H. Tolentino, E. Favre-Nicolin, and L. Ranno, *Phys. Rev. B* **70**, 174451 (2004).
- [15] Y. Joly, *Phys. Rev. B* **63**, 125120 (2001).